NANOSYSTEMS: PHYSICS, CHEMISTRY, MATHEMATICS, 2019, 10 (3), P. 235–242

Effect of periodic permeability of lung airways on the flow dynamics of viscous fluid

J. Kori*, Pratibha

Department of Mathematics, Indian Institute of Technology Roorkee, Roorkee-247667, Uttarakhand, India

*jyotikorii@gmail.com

DOI 10.17586/2220-8054-2019-10-3-235-242

In this study, we aimed to find the effect of periodic permeability on the flow dynamics of an incompressible, Newtonian, viscous and pulsatile flow of air flowing through airway generations 5–10. To solve this problem, we used a generalized Navier Stokes equation by including the Darcy law of a porous media with periodic permeability for the flow of air and Newton equation of motion for the flow of nanoparticles. The finite difference explicit numerical scheme has been carried out to solve the governing nonlinear equations and then computational work is done on MATLAB R2016 by user defined code. After performing numerical computation we found by varying mean permeability of porous media velocity of air and particle increased gradually with axial and radial distance respectively.

Keywords: lung generation, deposition, periodic permeability, pulsatile flow, nanoparticle.

Received: 22 May 2019

Revised: 6 June 2019

1. Introduction

Every day billions of particles are inhaled with the ambient air [1, 2]. Concerning the effect of inhaled particulate matter on different regions of human lung, a number of studies are done. Tian et al. [3] stated that nanoparticles of range 5.52–98.2 nm pose risks for occupational workers and are the cause of various respiratory, cardiovascular, and neurological disorders. A study based base on CT scanner images carried out by Debo et al. [4] to find the effect of micron particles (1–10 μm) and nanoparticles (1–100 nm) in the nasal cavity up to the upper six-generation of the lung has observed that the deposition efficiency of micron particles there is much higher than nanoparticles in the nasal region. A theoretical study by Sturm [5] states that due to very small size, nanoparticles are aggregates with highly irregular shape (chain-like, loose, compact) and that these particles are taken after inhalation up into the respiratory tract by the mechanism of Brownian diffusion, sedimentation [6] and are then stored in the epithelial cells for a longer time span, which causes the formation of cancerous cells. Recently, Saini et al. [7] studied the deposition of nanoparticles of diameter 100 nm and found that these particles travel deeper into the lung and ultimately deposit in the alveolar ducts of the human lung.

According to Haber et al. [8] the deposition of particles also depends on media porosity due to the large number of alveoli inside the human lung. Many researchers [9, 10] defined it as a sponge or porous medium. Cheng [11] and Vafai et al. [12] used the porous media approach for convective mass transfer in the airway and its surrounding wall tissue. Also, Kuwahara et al. [13] obtained mass transfer resistance between the inlet of the trachea and the blood in the capillaries using the porous media approach. Saini et al. [14] treated the alveolar region as a biofilter and found removal efficiency of lung for nanoparticles by using generalized Navier-Stokes equations. Recently DeGroot and Straatman [9] worked on expansion and contraction of alveolar duct and assumed lung is a porous medium by using theory of volume-averaging technique for unit cell of an alveolar duct to predict permeability of human lung.

Based on our literature review we found that there are a few studies which considered the lung as a porous medium. Those studies which took this point of view, however, assumed either that the permeability depends on the porosity or that it is constant. Thus, we aimed to study the effect of periodic permeability on the two dimensional pulsatile flow of viscous air flowing through airway generations 5–10 due to periodic breathing. The governing nonlinear equations are described in detail and then solved numerically by using finite difference methods. The computational work was carried out using MATLAB 2016 through a user defined code.

2. Mathematical modeling

2.1. Physical configuration

To understand the flow regime within airway generations 5–10, an extended horizontal circular cylindrical tube (representing an airway tube) of the circular cross section is considered whose radius is ‘b’ and is placed perpendicularly to the incoming flow [15]. A schematic diagram is shown in Fig. 1, where, ‘z’ is the axial direction of flow and ‘r’ is the radial direction of flow.

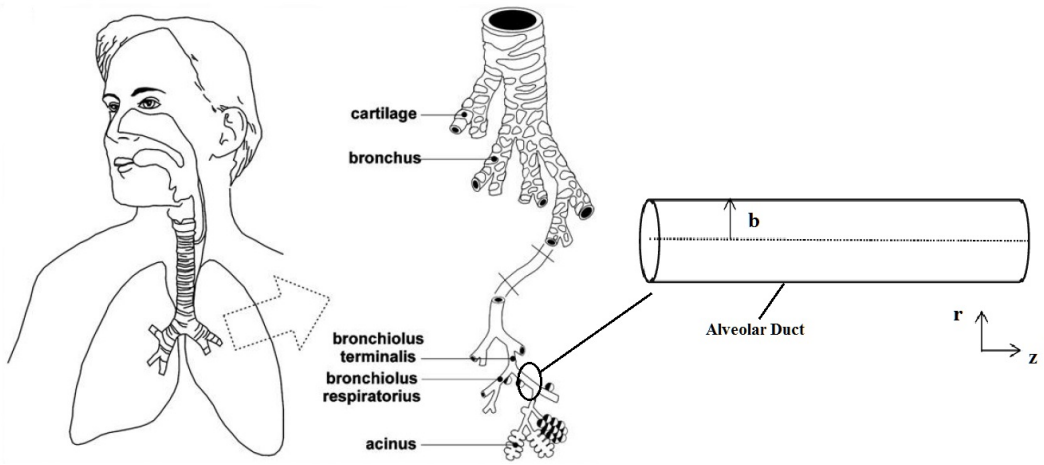

FIG. 1. Cross sectional view of airway duct (circular cylindrical tube) of a tracheobronchial tree [16], where 'r' is the radial direction and 'z' is the axial direction of viscous air flow

2.2. Governing equations for viscous air flowing through airway tube

We assumed that an incompressible, laminar, unsteady, axi-symmetric, Newtonian and fully-developed fluid is flowing along the axis of the circular tube with time dependent sinusoidal pressure gradient. The tissue of the airway tube is approximated as a homogeneous porous medium, which is viewed as a continuum, and saturated with an incompressible fluid. A mathematical model proposed by Saini et al. [7] is taken under consideration by using Darcy low of porous media together with the periodic permeability of the medium in order to find their effect on the flow of fluid [1]. The corresponding two dimensional conservation equations of mass, momentum together with particle motion in the cylindrical polar coordinates system (r, z) for symmetrical flow (θ = constant) which satisfy our assumptions are given below:

First, there is the equation of continuity, given by:

$$\frac{\partial u_r}{\partial r} + \frac{u_r}{r} + \frac{\partial u_z}{\partial z} = 0. \tag{1}$$

$$\frac{\partial v_r}{\partial r} + \frac{v_r}{r} + \frac{\partial v_z}{\partial z} = 0. \tag{2}$$

Secondly there is the equation of radial momentum, given by:

$$\frac{\partial u_r}{\partial t} + \frac{u_r}{\epsilon}\frac{\partial u_r}{\partial r} + \frac{u_z}{\epsilon}\frac{\partial u_r}{\partial z} = -\frac{\epsilon}{\rho_a}\frac{\partial p}{\partial r} + \nu\left(\frac{\partial^2 u_r}{\partial r^2} + \frac{1}{r}\frac{\partial u_r}{\partial r} + \frac{\partial^2 u_r}{\partial z^2}\right) + k_f\frac{\rho_p}{\rho_a}(v_r - u_r) - \frac{\epsilon\nu}{K}u_r. \tag{3}$$

Finally we have the equation of axial momentum, given by:

$$\frac{\partial u_z}{\partial t} + \frac{u_r}{\epsilon}\frac{\partial u_z}{\partial r} + \frac{u_z}{\epsilon}\frac{\partial u_z}{\partial z} = -\frac{\epsilon}{\rho_a}\frac{\partial p}{\partial z} + \nu\left(\frac{\partial^2 u_z}{\partial r^2} + \frac{1}{r}\frac{\partial u_z}{\partial r} + \frac{\partial^2 u_z}{\partial z^2}\right) + k_f\frac{\rho_p}{\rho_a}(v_z - u_z) - \frac{\epsilon\nu}{K}u_z. \tag{4}$$

where, ϵ is the porosity of lung and K is the permeability of porous medium. We also have the equations for the particle motion. In the radial direction, we have:

$$\frac{\partial v_r}{\partial t} + v_z\frac{\partial v_r}{\partial z} + v_r\frac{\partial v_r}{\partial r} = \frac{k_f(u_r - v_r)}{m}. \tag{5}$$

In the axial direction, we have:

$$\frac{\partial v_z}{\partial t} + v_z\frac{\partial v_z}{\partial z} + v_r\frac{\partial v_z}{\partial r} = \frac{k_f(u_z - v_z)}{m}. \tag{6}$$

$$k_f = 3\pi\mu d.$$

[1]Henry Darcy was a French engineer who gave a mathematical relationship between permeability and velocity of media, which is known as Darcy law of porous media [17]

2.3. Assumption

There is no radial flow along the axis of the airway duct and the axial velocity gradient of the streaming air may be implicit to be equal to zero:

$$u_r = 0, v_r = 0, \frac{\partial u_z}{\partial r} = 0, \frac{\partial v_z}{\partial r} = 0. \tag{7}$$

2.4. Initial and boundary condition

- At rest $t \leq 0$, no flow takes place therefore,

$$u_r = v_r = u_r = v_r = 0, \tag{8}$$

The boundary conditions for $t > 0$ are given as follows,

- Due to periciliary liquid layer, no-slip condition is forced at the inner surface of the wall:

$$u_r = 0, u_z = 0, v_r = 0, v_z = 0. \tag{9}$$

3. Methodology

3.1. Transformation of the governing equations

In order to solve the equations numerically we have to make the above equations dimensionless by using following quantities:

$$R^* = \frac{r}{b}, Z^* = \frac{z}{b}, p^* = \frac{P}{\rho_a U_0^2}, \tau^* = \frac{tU_0}{b}, U_r^* = \frac{u_r}{U_0}, U_z^* = \frac{u_z}{U_0}, V_r^* = \frac{v_r}{U_0}, V_z^* = \frac{v_z}{U_0},$$
$$Da = \frac{K}{b^2}, P_l = \frac{\rho_p}{\rho_a}, S_m = \frac{rk}{U_0}, Re = \frac{rU_0}{\nu}.$$

Finally, we obtain the following equations:

$$\frac{\partial U_r}{\partial R} + \frac{U_r}{R} + \frac{\partial U_z}{\partial Z} = 0. \tag{10}$$

$$\frac{\partial V_r}{\partial R} + \frac{V_r}{R} + \frac{\partial V_z}{\partial Z} = 0. \tag{11}$$

$$\frac{\partial U_z}{\partial \tau} + \frac{U_r}{\epsilon}\frac{\partial U_z}{\partial R} + \frac{U_z}{\epsilon}\frac{\partial U_z}{\partial Z} = -\epsilon\frac{\partial P}{\partial Z} + \frac{1}{Re}\left(\frac{\partial^2 U_z}{\partial R^2} + \frac{1}{R}\frac{\partial U_z}{\partial R} + \frac{\partial^2 U_z}{\partial Z^2}\right) + S_m P_l\left(V_z - U_z\right) - \frac{\epsilon}{DaRe}U_z. \tag{12}$$

$$\frac{\partial V_z}{\partial \tau} + V_r\frac{\partial V_z}{\partial R} + V_z\frac{\partial V_z}{\partial Z} = \frac{S_m\left(U_z - V_z\right)}{m}. \tag{13}$$

In equation 12, due to rhythmic breathing, expansion and contraction and the right heart pressure we assumed a non-dimensional time dependent sinusoidal pressure gradient inside airway duct as follows,

$$\frac{\partial P}{\partial Z} = -a_0 \sin\omega t, \quad \omega = 2\pi f \tag{14}$$

where f is the frequency of breathing. Also, in this equation, we assumed permeability, K, of media is periodic [18] due to an oscillation of velocity about a nonzero constant mean. So, K can be defined in non-dimensional form as

$$K = \frac{K_0}{1 - a_0 cos(\pi Z)}, \tag{15}$$

where, K_0 is the mean permeability of porous medium and a_0 is the amplitude of oscillation.

Also, transformed initial and boundary conditions together with assumptions respectively are as follows:

$$U_r = 0, U_z = 0, V_r = 0, V_z = 0. \tag{16}$$

$$U_r = 0, V_r = 0, U_z = 0, V_z = 0. \tag{17}$$

$$U_r = 0, \frac{\partial U_z}{\partial R} = 0, V_r = 0, \frac{\partial V_z}{\partial R} = 0 \tag{18}$$

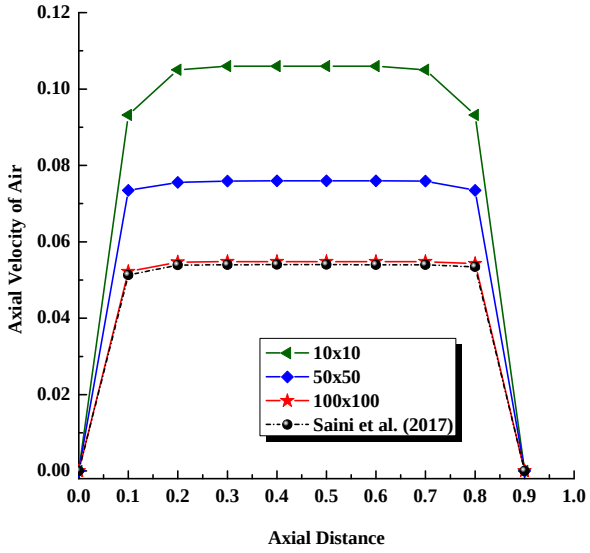

FIG. 2. A comparative result between published [7] and present work for axial velocity profile of air at $\tau = 0.9$, $R = 0$, $Z = [0, 1]$, $Re = 10$, $d = 100$ nm and $a = 125$ μm

4. Numerical scheme

Analytical approaches are suitable for linear problems, but the governing equations of the present issue are nonlinear. Consequently it is difficult to find the solution of these nonlinear equations subject to the initial and boundary conditions by an analytical approach. For this reason, we have adopted a numerical procedure to find solutions of the problem. Although there are various numerical techniques, for example, the finite difference method (FDM) [7,19–21], the finite element method (FEM) [10, 22] or the finite volume method (FVM) [23] have been used to solve such nonlinear problem. Among those methods, FDM is a basic and less tedious technique for regular geometry. Our problem is related to the flow in a circular cylinder, with a regular geometry. Thus, to solve the present problem we also applied finite difference numerical scheme. The discretization of the axial velocity $U(R, Z, \tau)$ is written as $U_z(R_i, Z_j, \tau)$ or $((U_z)_{i,j})^k$ and computational grid that has been used is of the following form:

$$\begin{aligned} R_i = i.\Delta R; \quad i = 0, 1, 2, ...M, R_M = 1.0, \\ Z_j = j.\Delta Z; \quad j = 0, 1, 2, ...N, \\ \tau_k = k.\Delta\tau; \quad k = 0, 1, 2, ...O. \end{aligned} \tag{19}$$

Where i, j and k are the space and time indices, and $\Delta R = 0.01$, $\Delta Z = 0.01$ and $\Delta\tau = 10^{-5}$ are increments in radial, axial and time respectively. We used central difference approximations, for all the spatial derivatives, as follows,

$$\frac{\partial U_z}{\partial Z} = \frac{(U_z)^n_{i,j+1} - (U_z)^n_{i,j-1}}{2\Delta Z}. \tag{20}$$

For the second order central difference approximation for the time and space derivatives we have used:

$$\frac{\partial^2 U_z}{\partial Z^2} = \frac{(U_z)^n_{i,j+1} - 2(U_z)^n_{i,j} + (U_z)^n_{i,j-1}}{(\Delta Z)^2}. \tag{21}$$

and for first order time derivative at point (R_i, Z_j, τ_k) we applied forward difference approximation as follows:

$$\frac{\partial (U_z)}{\partial \tau} = \frac{(U_z)^{n+1}_{i,j} - (U_z)^n_{i,j}}{2\Delta\tau}. \tag{22}$$

After applying the above mentioned discretization techniques, we have obtained velocity profiles at the $(j+1)^{th}$ time level in terms of the velocity at j^{th} time level for Equations (11)-(18) respectively.

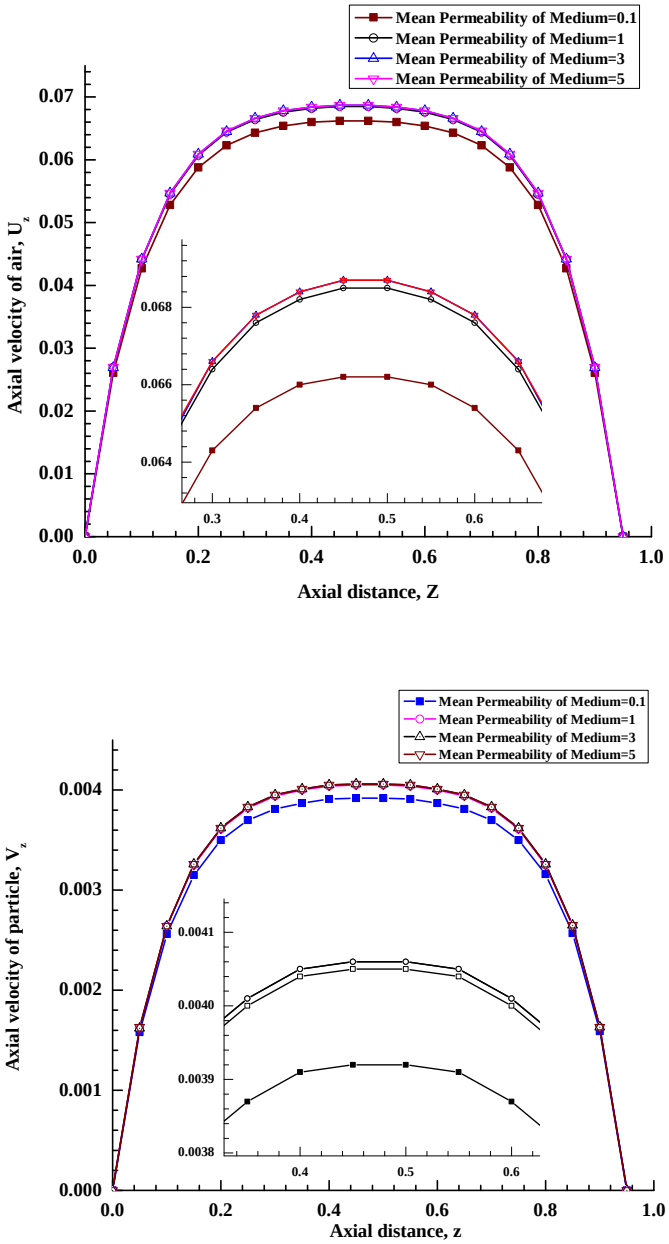

FIG. 3. Effect of mean permeability of porous media on axial velocity of (a) air and (b) particles at $\tau = 0.5$, $R = 0$, $Z = [0, 1]$, $Re = 10$, $d = 50$ nm, $a = 0.5$ μm

We used following stability criteria for explicit finite difference scheme and found our results are accurate of order 10^{-5} by using grid size $100\times100\times10^5$ (i.e. $M = 100$, $N = 100$, $O = 10^5$):

$$\max\left(\frac{\Delta\tau}{\Delta Z^2}\right) \leq 0.5. \tag{23}$$

4.1. Model Validation and Grid Independency Test

Before analyzing the problem related to periodic permeability and sinusoidal pressure gradient due to periodic breathing, a grid independency test, together with a numerical code validation to find the predictive accuracy of the mathematical model is done by comparing outcomes produced by present study with the study of Saini et al. [7] and shown in Fig. 2 for grid sizes $10\times10\times10^5$, $50\times50\times10^5$ and $100\times100\times10^5$. Saini et al. [7] performed an extensive

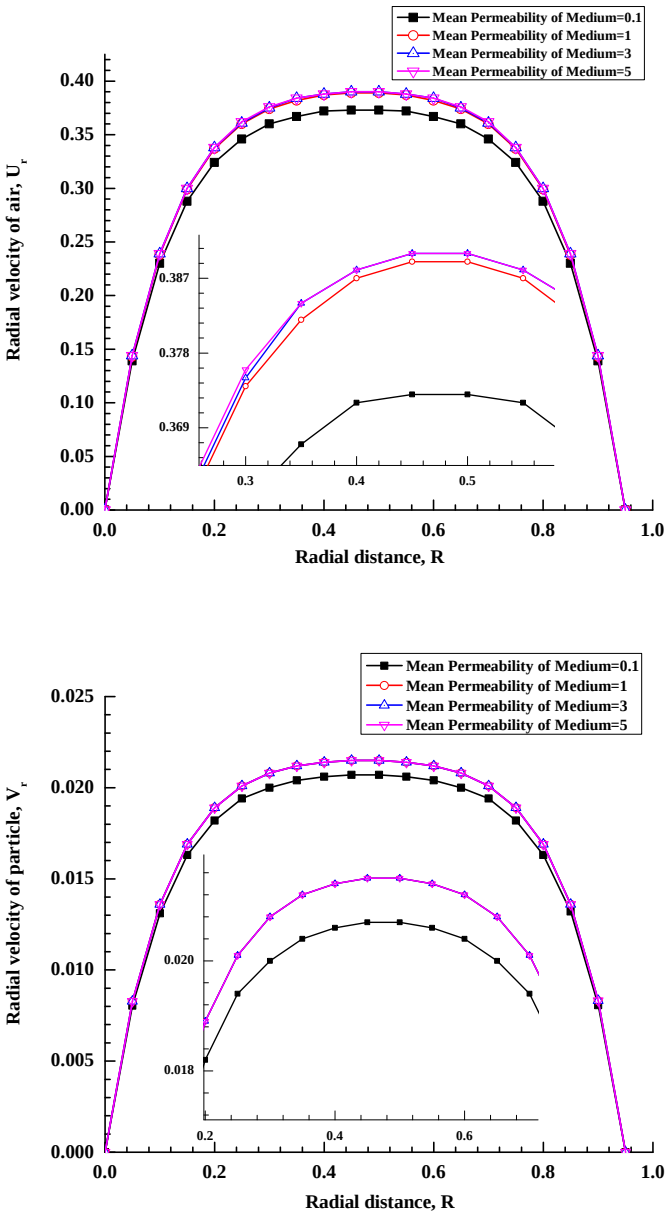

FIG. 4. Effect of mean permeability of porous media on radial velocity of (c) air and (d) particles at $\tau = 0.5$, $R = 0$, $Z = [0, 1]$, $Re = 10$, $d = 50$ nm, $a = 0.5$ μm

quantitative study through numerical computations to study the flow of viscous air in alveolar region and calculated the location of deposition of the nanoparticles of diameter=100 nm inside the alveolar duct of the human lung. All the results are presented in graphical form in both radial and axial directions at various time points. However, in their study authors did not consider porosity of alveolar region, which an important factor for biological tissues. So, in the present study we include porosity of media and used periodic permeability due to an oscillation of velocity about a nonzero constant mean.

We compared result of present study with the result of Saini et al. [7] in Fig. 2 for velocity of air with respect to axial distance at $\tau = 0.9$, $R = 0$, $Z = [0, 1]$ after removing porosity and relevant terms (Darcy term, periodic permeability) at $Re = 10$, $d = 100$ nm, and $a = 125$ μm. We found that our results did not change for grid size of $100\times100\times10^5$ and higher. Hence, a grid size of $100\times100\times10^5$ is chosen for all of our computations.

We compared result of present study with the result of Saini et al. [7] in Fig. 2 for velocity of air with respect to axial distance at $\tau = 0.9$, $R = 0$, $Z = [0, 1]$ after removing porosity and relevant terms (Darcy term, periodic permeability) at $Re = 10$, $d = 100$ nm, and $a = 125$ μm. We found that our results did not change for grid size of $100\times100\times10^5$ and higher. Hence, a grid size of $100\times100\times10^5$ is chosen for all of our computations.

5. Results and discussion

In this work we aimed to find the effect of periodic permeability of the porous lung on air and particle velocity by varying the mean permeability of medium. A numerical computation is done by using following values [7, 18, 24–27]:

$$m = 0.0002 \text{ Kg/l}, \quad d = 50 \text{ nm}, \quad f = 0.3 \text{ hz}, \quad \rho_a = 1.145 \text{ kg/m}^3, \quad \rho_p = 0.02504 \cdot 10^{12}\text{m}^{-3},$$
$$r = 0.5 \ \mu\text{m}, \quad a_0 = 1 \text{ Kg/m}^2\text{s}^2, \quad \nu = 1.71 \cdot 10^{-5} \text{ m}^2/\text{s}, \quad Re = 1 - 20, \quad \epsilon = 0.6, \quad K_0 = 0.1 - 5. \tag{24}$$

In Fig. 3, we obtained effect of periodic permeability of media by varying mean permeability K_0 of medium from 0.1 to 5 on axial velocity of air and particle at $\tau = 0.5$, $R = 0$, $Z = [0, 1]$, $Re = 10$, $d = 50$ nm, $a = 0.5$ μm respectively. We found from Fig. 3(a)–3(b), at $K_0 = 0.1$ the velocity of air and particle in axial directions are lesser than velocities at $K_0 = 5$. However, by increasing value of mean permeability (K_0) from 0.1 to 5 periodic permeability of airways increases and due to highly permeable walls, level of pressure inside airway tubes reduces, which increases velocity of air and particles in axial directions of flow periodically.

In Fig. 4, we obtained effect of periodic permeability of media by varying mean permeability K_0 of medium from 0.1 to 5 on radial velocity of air and particle at $\tau = 0.5$, $R = 0$, $Z = [0, 1]$, $Re = 10$, $d = 50$ nm, $a = 0.5$ μm respectively. We found from Fig. 4(a)–4(b), at $K_0 = 0.1$ velocity of air and particle in radial directions are lesser than velocities at $K_0 = 5$. However, by increasing the value of mean permeability (K_0) from 0.1 to 5 periodic permeability of airways increases and due to highly permeable walls, level of pressure inside airway tubes reduces, which increases velocity of air and particles in radial directions of flow periodically.

Consequently, we found that axial and radial velocity of air and particle influenced highly as compared to axial and radial velocity of particle and concluded that the increase in permeability, K_0, elevates airflow inside the lung airways.

6. Conclusion

A mathematical model characterizing the motion of nanoparticles, diameter 50 nm, with the laminar, sinusoidal flow of air through airway duct is developed. Porosity of tissue and periodic permeability of media due to rhythmic breathing is considered. It is found that periodic permeability affects the velocity of air and particles in axial and radial direction of flow such as the increment in the permeability of porous media, K_0, rises the flow of air inside the lung airways.

Acknowledgment

One of the authors, Jyoti Kori, is thankful to Ministry of Human Resource Development India (Grant Code:-MHR-02-23-200-44) for providing fund and support while writing this manuscript.

References

[1] Heyder J. Deposition of Inhaled Particles in the Human Respiratory Tract and Consequences for Regional Targeting in Respiratory Drug Delivery. *Proc Am Thorac Soc.*, 2004, P. 315-320.

[2] Kori J., Pratibha. Numerical Simulation of Dusty Air Flow and Particle Deposition Inside Permeable Alveolar Duct. *Int. J. Appl. Comput. Math*, 2019, **5**, P. 1–13.

[3] Tian L., Shang Y., Chen R., Bai R., Chen C., Inthavong K., Tu1 J. A combined experimental and numerical study on upper airway dosimetry of inhaled nanoparticles from an electrical discharge machine shop. *Particle and Fibre Toxicology*, 2017, **14**, P. 24.

[4] Li D., Xu Q., Liu Y., Libao Y., Jun J. *Numerical Simulation of Particles Deposition in a Human Upper Airway*. Advances in Mechanical Engineering, 2014.

[5] Sturm R. Theoretical deposition of carcinogenic particle aggregates in the upper respiratory tract. *Ann Transl Med.*, 2013, **1**, P. 25.

[6] Sturm R. A computer model for the simulation of nanoparticle deposition in the alveolar structures of the human lungs. *Ann Transl Med.*, 2015, **3**, P. 281.

[7] Saini A., Katiyar V.K., Pratibha. Two-dimensional model of nanoparticle deposition in the alveolar ducts of the human lung. *Applications & Applied Mathematics*, 2017, **12**, P. 305–318.

[8] Haber S., Yitzhak D., Tsuda A. Gravitational deposition in a rhythmically expanding and contracting alveolus. *J. Appl. Physiol.*, 2013, **95**, P. 657–671.

[9] DeGroot C.T., Straatman A.G. A porous media model of alveolar duct flow in the human lung. *Journal of Porous Media*, 2018.

[10] Khanafer K., Cook K., Marafie A. The Role of Porous Media in Modeling Fluid Flow Within Hollow Fiber Membranes of The Total Artificial Lung. *J. Porous Media*, 2012, **15**, P. 113–122.

[11] Cheng P. Heat Transfer in Geothermal Systems. *Advances in Heat Transfer*, 1979, **14**, P. 1–105.

[12] Vafai K., Tien C.L. Boundary and Inertia Effects on Flow and Heat Transfer in Porous Media. *Int. J. Heat Mass Transfer*, 1981, **24**, P. 195–203.

[13] Kuwahara F., Sano Y., Liu J., Nakayama A. A Porous Media Approach for Bifurcating Flow and Mass Transfer in a Human Lung. *J. Heat Transfer*, 2009, **131**, P. 101013-5.
[14] Saini A., Katiyar V.K., Pratibha. Numerical simulation of gas flow through a biofilter in lung tissues. *World Journal of Modelling and Simulation*, 2015, **11**, P. 33–42.
[15] Balashazy I., Hofmann W., Farkas A.,, Madas B.G. Three-dimensional model for aerosol transport and deposition in expanding and contracting alveoli. *Inhalation Toxicology*, 2008, **20**, P. 611–621.
[16] Sturm R., Hofmann W. A theoretical approach to the deposition and clearance of fibers with variable size in the human respiratory tract. *J. of Hazardous Materials*, 2009, **170**, P. 210–218.
[17] Darcy H. *Les Fontaines Publiques de la Ville de Dijon*. Dalmont, Paris, 1856.
[18] Singh K.D., Verma G.N. Three-Dimensional Oscillatory Flow through a Porous Medium with Periodic Permeability. *Z. Angew. Math. Mech.*, 1995, **75**, P. 599–604.
[19] Kori J., Pratibha. Numerical Simulation of Mucus Clearance inside Lung Airways. *Journal of Applied Fluid Mechanics*, 2018, **11**, P. 1163–1171.
[20] Kori J., Pratibha. Simulation and Modeling for Aging and Particle Shape Effect on Airflow Dynamics and Filtration Efficiency of Human Lung, *Journal of Applied Fluid Mechanics*, 2019, **12**, P. 1273–1285.
[21] Smith S., Cheng U.S., Yeh H.C. Deposition of ultrafine particles in human tracheobronchial airways of adults and children. *Aerosol Sci. Tech.*, 2010, **35**, P. 697–709.
[22] Seraa T., Uesugib K., Yagib N., Yokotac H. Numerical simulation of airflow and microparticle deposition in a synchrotron micro-CT-based pulmonary acinus model. *Computer Methods in Biomechanics and Biomedical Engineering*, 2013, **18**, P. 1427-1435.
[23] Koullapis P.G., Kassinos S.C., Bivolarova M.P., Melikov A.K. Particle deposition in a realistic geometry of the human conducting airways: Effects of inlet velocity profile, inhalation flowrate and electrostatic charge. *J Biomech.*, 2016, **49**(11), P. 2201–2212.
[24] Ismail Z., Abdullah I., Mustapha N., Amin N. A power-law model of blood flow through a tapered overlapping stenosed artery. *Appl. Math. Comput.*, 2007, **195**, P. 669–680.
[25] Kapur J.N. *Mathematical Models in Biology and Medicine*. East-West Press, Pvt. Ltd., New Delhi, 1985.
[26] Mandal P.K. An unsteady analysis of non-Newtonian blood flow through tapered arteries with a stenosis. *Int. J. Non-Linear Mech.*, 2005, **40**, P. 151–164.
[27] Singh P., Misra J.K., Narayan K.A. Free convection along a vertical wall in a porous medium with periodic permeability variation. *Int. J. Numer. Anal. Methods Geomech.*, 1989, **13**.

Appendix

Nomenclature is defined in Table 1.

TABLE 1. Nomenclature

Variable	Description	Variable	Description
r	radial direction of flow	z	axial direction of flow
u_r	air velocity radial direction	v_r	particle velocity radial direction
u_z	air velocity axial direction	v_z	particle velocity axial direction
ρ_p	density of particles	ρ_a	density of air
ν	kinematic viscosity	k_f	Stokes drag force
K	permeability of tissue	K_0	Mean permeability of medium
P_l	particle load	Da	Darcy number
a_0	amplitude	f	breathing frequency
μ	dynamics viscosity	Re	Reynolds number
t	time	ϵ	media porosity
d	diameter of spherical particle of unite density		